Precision laser micromachining of trenches in GaN on sapphire

G. Y. Mak, E. Y. Lam, and H. W. Choi[a]
Department of Electrical and Electronic Engineering, The University of Hong Kong, Pokfulam Road, Hong Kong, China

(Received 1 October 2009; accepted 8 February 2010; published 26 March 2010)

Trench formation for device isolation on GaN light-emitting diode (LED) wafers via nanosecond ultraviolet laser micromachining is demonstrated. Trenches with smooth sidewalls and flat bottom surfaces are produced. Unlike wafer scribing with laser beams, the formation of trenches requires that the incident fluence is sufficient for laser ablation of GaN, yet low enough to prevent ablation of the sapphire substrate. Owing to the dissimilar ablation thresholds between GaN and sapphire, the etch process terminates automatically at the GaN/sapphire interface. The effect of the following parameters on the trench properties and quality has been investigated: focus offset, pulse energy, pulse repetition rate, scan speed, and the number of scan passes. It was found that optimal focus offset and pulse energy, a high pulse repetition rate, and single cycle of slow scanning are the key factors for obtaining a trench with tapered sidewall and smooth bottom surface, which is suitable for the laying of interconnects conformally across the trench for device interconnection. This technique has been successfully applied to the rapid prototyping of interconnected LED arrays on a single chip, where metal interconnects run continuously across the micromachined trenches to connect the individual LED devices. © *2010 American Vacuum Society.* [DOI: 10.1116/1.3359593]

I. INTRODUCTION

The III-V wide band gap semiconductor gallium nitride (GaN) has been widely adopted for fabricating optoelectronic and electronic devices such as light-emitting diodes (LEDs),[1] laser diodes,[2,3] photodetectors,[4] and high-frequency transistors.[5,6] Despite the lattice mismatch, GaN is often grown as an epitaxial layer on sapphire substrates.[7] In order to fabricate multiple electrically isolated devices on a wafer, selective-area complete removal of GaN, such as the formation of deep trenches terminating at the GaN/sapphire interface, is an indispensable process step. As GaN is a hard material that is highly resistant to wet etch, dry etch is the conventional technique for achieving this purpose. Inductively coupled plasma etching, for example, offers an attractive etch rate of up to 1 μm/min.[8] However, etch selectivity is another major factor that limits the effectiveness of dry etching in creating high-aspect-ratio features. Typically, with photoresist as an etch mask, the highest etch selectivity that can be achieved is ~1:1.[9] As the typical thickness of a complete LED structure (comprising *p*-GaN, InGaN/GaN multiquantum wells and *n*-GaN layers) is 3–4 μm, a layer of photoresist of equal thickness has to be spin coated. Nevertheless, handling of thick photoresist layers is often cumbersome (such as edge bead effects[10]), coupled with the fact that thicker photoresists generally offer lower resolutions. The etch selectivity improves to ~1:4 if a hard mask such as SiO_2 is used, although additional photolithography and dry etch steps are required to pattern the hard mask. Therefore, developing a maskless direct-write deep etch technique for GaN materials is most desirable, particularly for rapid device prototyping.

In this article, we introduce an ultraviolet (UV) nanosecond laser micromachining technique for the formation of deep trenches in GaN films, suitable for device isolation on GaN LED wafers. When a sample is irradiated by a pulsed laser beam, and that the laser fluence (pulse energy divided by irradiated area) exceeds the ablation threshold of the surface material, a range of features including holes and trenches can be formed by translating the beam or the sample.[11] According to the findings of two previous published papers, the ablation threshold of GaN is 0.25 J/cm^2,[12] whereas that of sapphire is 4.5 J/cm^2 (Ref. 13) due to their large difference in absorption coefficient at UV wavelengths. If the laser fluence can be controlled to a level between these two ablation thresholds, the GaN layer will be ablated while the sapphire substrate is left intact; this forms the basis of our present work. It is imperative to reiterate that the conditions for trench formation in GaN on sapphire is rather different from laser scribing, whereby both the GaN and sapphire layers are to be ablated to complete separation.

Figure 1 illustrates how such control of laser fluence can be achieved through focus offset adjustment. In the vicinity of the focal point (best focus), the laser energy is concentrated into a tiny spot determined by beam quality and focusing optics so that the laser fluence is high enough to cut through both the GaN and sapphire layers. This is the mode of operation for LED die separation, as depicted in Fig. 1(a), whereby a cut as deep as possible is desired. As the sample is translated vertically to attain a larger focus offset, the laser spot on the sample surface is enlarged and the laser fluence is reduced. Upon careful adjustment, a range of focus offset planes can be found such that the laser fluence is just sufficient to ablate GaN but not sapphire. This "autostop" mechanism allows trenches with tapered sidewall and flat bottom surface to be formed [Fig. 1(b)], with controllable trench

[a]Electronic mail: hwchoi@hku.hk

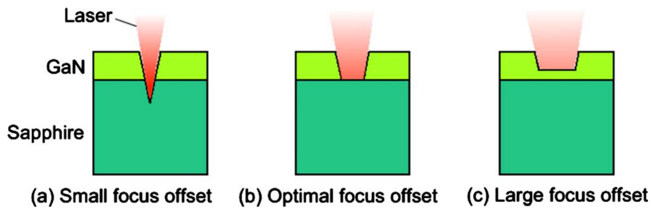

FIG. 1. (Color online) Principle of laser micromachining of trenches on GaN/sapphire material.

width. If the focus offset is further increased, the laser fluence will not be sufficient for ablating the whole layer of GaN, leaving a shallow trench on the surface [Fig. 1(c)].

In our experiments, five parameters including focus offset, pulse energy, pulse repetition rate, scan speed, and number of scan passes are varied in order to observe their influence on the trench quality. Roughening of the trench base or sidewall is often caused by melting and resolidification of the semiconductor material associated with the high temperatures induced by the nanosecond pulses. Although such localized heating effects can be avoided by the use of laser pulses with shorter pulse durations (picosecond or femtosecond), nanosecond lasers are by far the most affordable and flexible laser system that is suitable for general adoption. By enclosing a region with laser-micromachined trenches, GaN mesa structures can thus be formed. This technique is suitable for the rapid prototyping of devices,[14] whereby only a small area needs to be processed each time.

II. EXPERIMENTAL DETAILS

A schematic of the laser micromachining setup is shown in Fig. 2. The laser source used was a third-harmonic neodymium-doped yttrium lithium fluoride diode-pumped solid-state laser (Spectra Physics). The center wavelength is 349 nm and the pulse repetition rate can range from single pulse to 5 kHz. The nominal pulse duration is 4 ns, while the pulse energy can be varied by changing the diode pumping current. The expanded and collimated beam was guided by several laser mirrors and focused onto a piece of GaN LED sample (emission wavelength is 470 nm, thickness of GaN layer $\sim 3\ \mu$m) placed horizontally on an x-y motorized stage. The fused-silica focusing triplet lens allows UV and visible light to pass through and has a focal length of 19 mm. As the stage translates while keeping the laser spot station-

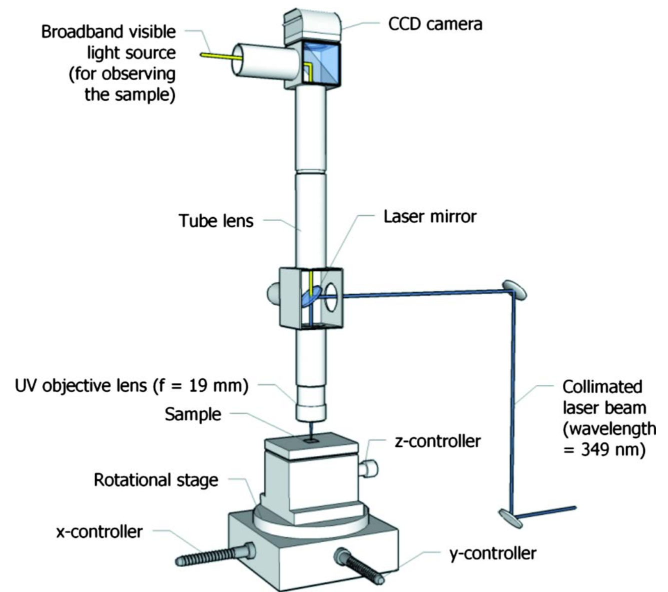

FIG. 2. (Color online) Schematic of the laser micromachining setup.

ary, trenches can be scribed onto the sample. The scan speed is controlled by software with a precision up to 25 μm/s. In order to shift the sample away from the focal point, the stage height can be manually adjusted relative to the best focus position. The accuracy of height adjustment is $\pm 5\ \mu$m. A charge-coupled device camera was installed confocal to the optical path for real-time observation of the micromachining process.

Owing to the high temperature during laser ablation, sedimentary by-products are formed on the surface of GaN.[15,16] These substances were effectively removed by sonification of the sample in dilute hydrochloric acid (HCl) (18% by mass) for 15 min. The sample was then rinsed in de-ionized water to remove remaining acid. The scanning electron microscope (SEM) images were acquired using a Hitachi S4800 SEM system, while the atomic force microscope (AFM) images were measured with a Seiko Instrument Nanopics system.

III. RESULTS AND DISCUSSION

Figures 3(a)–3(c) show SEM images of micromachined trenches at three different focus offset levels while keeping

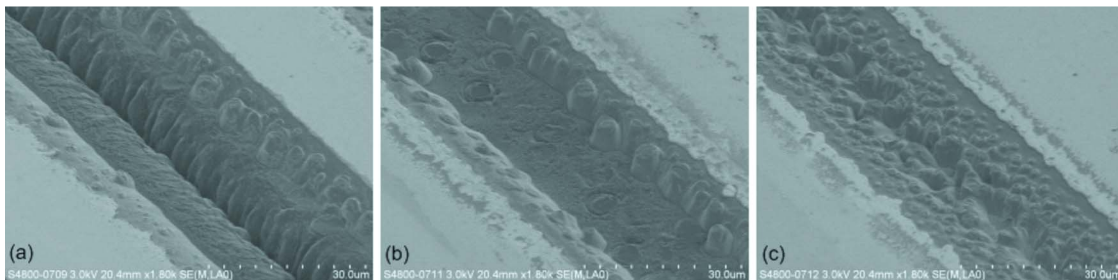

FIG. 3. (Color online) SEM images of trenches laser micromachined at different focus offset planes: (a) small offset of −300 μm; (b) optimal offset of −450 μm; (c) large offset of −600 μm. The pulse energy, pulse repetition rate, and scan speed are fixed at $\sim 23\ \mu$J, 1 kHz, and 25 μm/s, respectively.

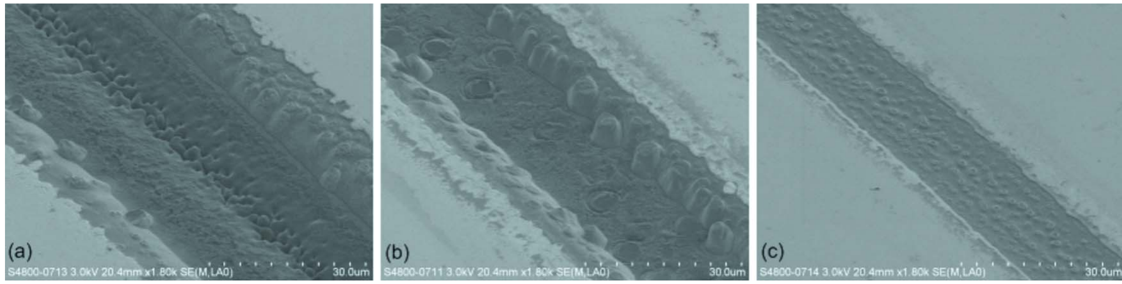

FIG. 4. (Color online) SEM images of trenches under different pulse energy: (a) higher pulse energy of 45 μJ; (b) optimal pulse energy of 23 μJ; (c) lower pulse energy of 7 μJ. The focus offset level, pulse repetition rate, and scan speed are fixed at −450 μm, 1 kHz, and 25 μm/s, respectively.

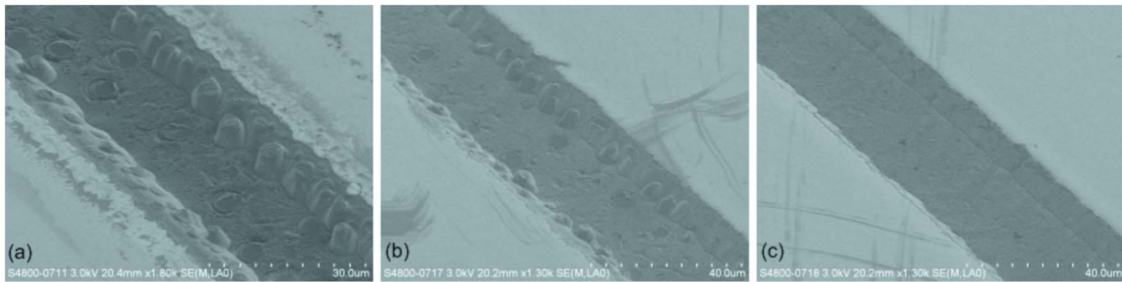

FIG. 5. (Color online) SEM images of trenches under different pulse repetition rate: (a) 1 kHz; (b) 3 kHz; (c) 5 kHz. The focus offset, pulse energy, and scan speed are fixed at −450 μm, 23 μJ, and 25 μm/s, respectively.

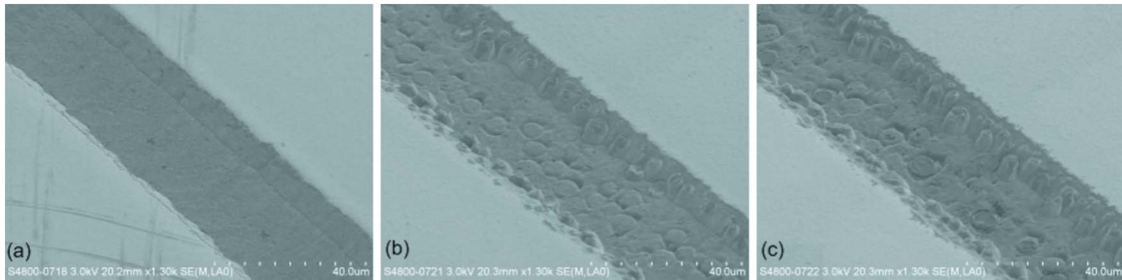

FIG. 6. (Color online) SEM images of trenches under different scan speeds: (a) 25 μm/s; (b) 75 μm/s; (c) 125 μm/s. The focus offset, pulse energy, and repetition rate are kept at −450 μm, 23 μJ, and 5 kHz, respectively.

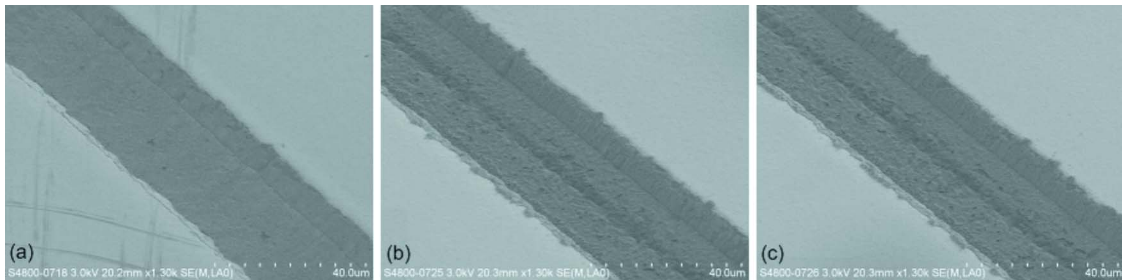

FIG. 7. (Color online) SEM images of trenches under different number of scans: (a) single pass; (b) three passes; (c) five passes. The focus offset, pulse energy, repetition rate and scan speed are maintained at −450 μm, 23 μJ, 5 kHz, and 25 μm/s, respectively.

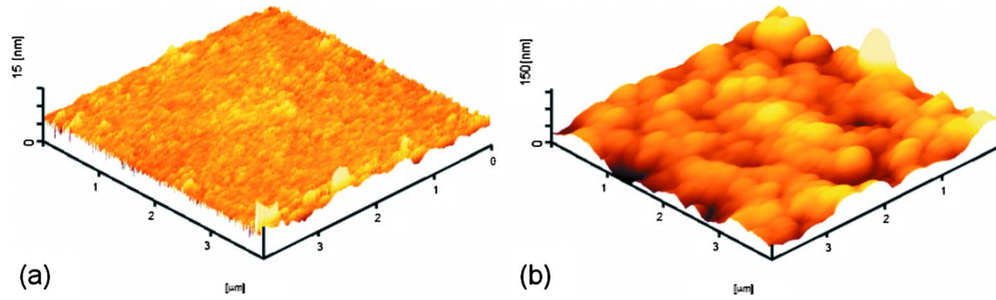

FIG. 8. (Color online) AFM images of (a) unprocessed sapphire substrate; (b) the bottom of a trench under optimal conditions: focus offset of −450 μm, pulse energy of 23 μJ, pulse repetition rate of 5 kHz, scan speed of 25 μm/s, and single pass.

the pulse energy, repetition rate, and scan speed constant. The focus offset level is defined as the distance shifted away from the focal plane, downward as positive. In Fig. 3(a) where the sample is positioned near the focal plane (−300 μm from focal plane), the laser beam ablates both the GaN and sapphire layers. A V-shaped valley is formed in the sapphire layer due to the Gaussian beam shape. Although trenches like these serve the purpose of electrical isolation between adjacent devices, the deep V-shaped valley is not suitable for the subsequent deposition of metal interconnect across the trench, which is crucial in interconnected device structures, such as interconnected light-emitting diode arrays. The metal interconnect will become discontinuous at the sharp corners of the valleys. At the optimal focal offset plane of −450 μm, as shown in Fig. 3(b), the ablation terminates automatically at the GaN/sapphire interface as the laser fluence drops below the ablation threshold value for sapphire, resulting in a flat and smooth sapphire bottom surface being exposed. At a larger focus offset plane of −600 μm, the GaN layer is not completely removed, leaving a shallow and rugged trench on the surface [Fig. 3(c)].

The SEM images in Figs. 4(a)–4(c) illustrate laser-micromachined trenches processed at three different pulse energies between 7 and 45 μJ, while keeping all other pa-

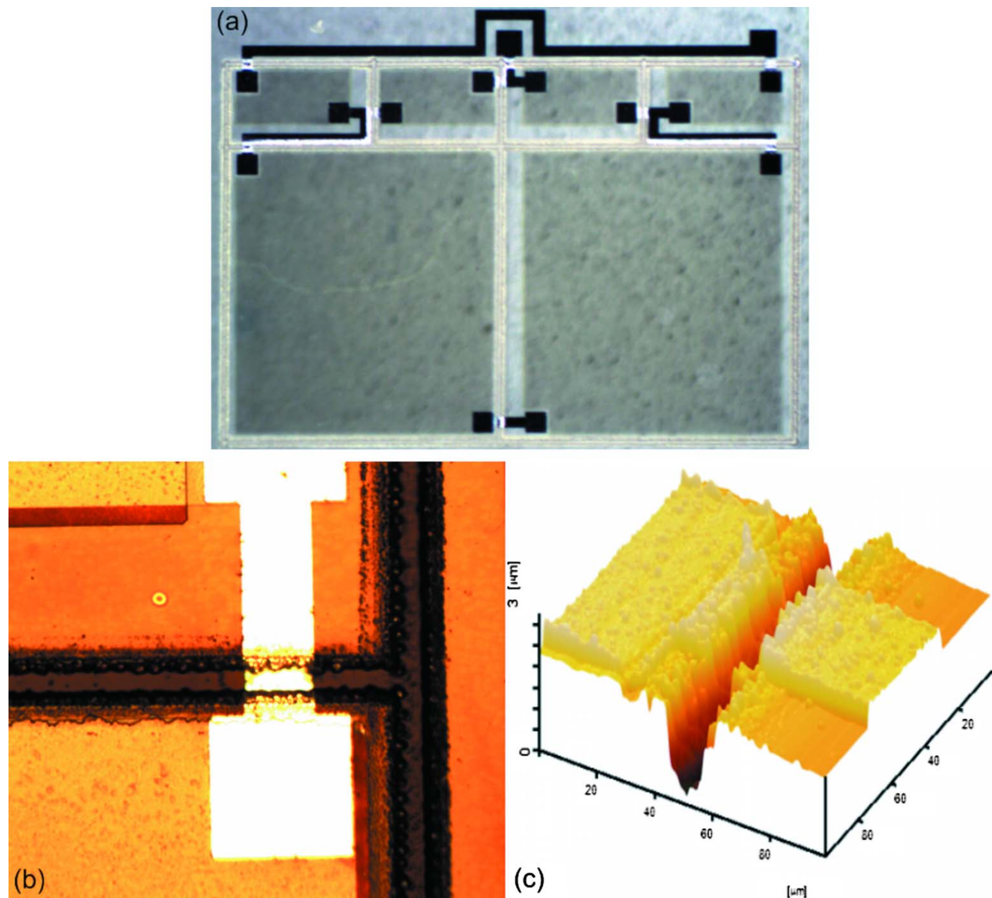

FIG. 9. (Color online) (a) Alternating-current LED: An example of an interconnected LED array. (b) Optical microscope image of a 500 nm Ti/Al interconnect deposited across a laser-micromachined trench. (c) AFM image of the same metal interconnect across the micromachined trench.

rameters constant. The focus offset is kept at the optimal value of −450 μm, as determined from the previous set of experiment. When the pulse energy is set too high, the effect is similar to that of having a smaller focus offset, whereby the GaN as well as sapphire are ablated to form a V-shaped trench [Fig. 4(a)]. Similar correspondence between low pulse energy and large focus offset can be observed in Fig. 4(c).

We can estimate the diameter of the irradiated region (assuming circular) required in our experiment. Assuming that the average pulse energy applied is 23.5 μJ and the ablation thresholds of GaN and sapphire are the values given in Sec. I, the laser fluence F has to satisfy the following condition:

$$0.25 < F < 4.5. \quad (1)$$

From this condition, the required diameter is between 26 and 109 μm. In order to remove the GaN completely without damaging the sapphire, the diameter of the irradiated region thus has to be as close to 26 μm as possible. This value correlates well with the width of the trench shown in Fig. 4(b), which is measured to be 20.74 μm.

Trenches that are laser micromachined under an increasing pulse repetition rate are shown in the SEM images of Figs. 5(a)–5(c); all other parameters are kept constant. It is observed that when the pulse repetition rate increases from 1 to 5 kHz, the trench width remains more or less unchanged, but the sidewall and bottom surface become increasingly smoother. Formation of stalagmite GaN structures rarely occurs. This observation can be understood in terms of heat accumulation effects and its consequence to the etch efficiency. As the repetition rate increases, cumulative heating by earlier pulses causes localized melting of the material.[17] The average surface temperature of the sample ($\bar{T}_n$) after being irradiated by a succession of n pulses is given by[18]

$$\bar{T}_n \approx 2T_m\left(\frac{t_p}{t_{pp}}\right)^{1/2}, \quad (2)$$

where T_m is the maximum surface temperature at the end of the first pulse, t_p is the pulse duration, and t_{pp} is the time between the end of a pulse and the start of the next pulse. As pulse repetition rate increases while keeping t_p and pulse energy unchanged, T_m stays constant and t_{pp} decreases. This results in an increase in the average surface temperature and thus the removal rate of the ablated materials, minimizing redeposition of debris over the trench.

The rate at which the laser beam scans across the material is also investigated. From Figs. 6(a)–6(c), it is observed that a faster translation rate does not result in a change in the trench width. However, it leads to degradation in the trench quality. Decomposition and melting become more severe and stalagmitelike structures begin to appear around the sidewalls. If the scan speed is increased further, ablation of the GaN layer will not be complete since the total number of photons incident at a particular region decreases when the scan speed increases and the pulse repetition rate is kept constant.

The remaining factor to consider is the number of scans. Similar to the effect of increasing scan speed, an increase in the number of scans does not alter the trench width. However, a narrow groove is formed in the center of the trenches for three and five passes, as illustrated in Figs. 7(b) and 7(c), respectively. There is also no remarkable improvement in the sidewall and bottom surface quality.

From the above sets of experiments, we can develop the conditions for laser micromachining of an optimal trench, which can be obtained by tuning the focus offset level, pulse energy, pulse repetition rate, scan speed, and the number of scan cycles. Figures 8(a) and 8(b) show AFM surface scans of an unprocessed sapphire substrate and the bottom of a trench micromachined at optimal conditions, respectively. The rms roughness of the trench has risen to 16.01 nm compared to that of the unprocessed sapphire at 0.7827 nm, which is still reasonably smooth. One of the major applications of this laser micromachining technique is the rapid prototyping of interconnected LED arrays on a single chip. An example of such a device is the alternating-current LED, as shown in Fig. 9(a), whereby the device consists of multiple interconnected LEDs, which form the rectifying circuit and the emissive components. Details of this device will be reported elsewhere. In order to interconnect the LEDs in an array, trenches must be formed between the mesa regions of individual devices. The trenches must have smooth and inclined sidewalls for conformal coverage of the metal interconnects. The technique of laser micromachining serves this purpose particularly for rapid prototyping, and even large scale processing with high-repetition-rate lasers. Figures 9(b) and 9(c) illustrate a 500 nm thick Ti/Al bilayer interconnect being deposited across a laser-micromachined trench. The deposition was performed by electron-beam evaporation. The LEDs are electrically isolated from each other by the trenches, and connected in series by the Ti/Al interconnect (with an underlying SiO_2 layer for isolation). The smooth tapered sidewall and flat bottom allow the Ti/Al layer to run smoothly across the trenches.

IV. CONCLUSION

Laser-micromachined trenches in GaN/sapphire wafers with smooth sidewalls and flat bottom surfaces using nanosecond UV pulses are demonstrated. When process conditions are optimized, laser ablation terminates automatically at the GaN/sapphire interface, making use of the difference in ablation thresholds of GaN and sapphire. Several parameters that affect the trench quality have been investigated. The optimal conditions derived from our experiments are focus offset of −450 μm, pulse energy of 23 μJ, pulse repetition rate of 5 kHz, and scan speed of 25 μm/s. The process has been successfully applied to the interconnection of LED arrays on a single chip.

[1]I. Akasaki and H. Amano, Jpn. J. Appl. Phys., Part 1 **45**, 9001 (2006).
[2]S. Nakamura, M. Senoh, S. Nagahama, N. Iwasa, T. Yamada, T. Matsushita, H. Kiyoku, and Y. Sugimoto, Jpn. J. Appl. Phys., Part 2 **35**, L74 (1996).
[3]Y. D. Lin *et al.*, Appl. Phys. Express **2**, 082102 (2009).
[4]D. G. Zhao, D. S. Jiang, J. J. Zhu, Z. S. Liu, S. M. Zhang, and H. Yang, Semicond. Sci. Technol. **23**, 095021 (2008).
[5]M. Asif Khan, J. N. Kuznia, A. R. Bhattarai, and D. T. Olson, Appl. Phys.

Lett. **62**, 1786 (1993).
[6]S. Keller, Y. F. Wu, G. Parish, N. Zhang, J. J. Xu, B. P. Keller, S. P. DenBaars, and U. K. Mishra, IEEE Trans. Electron Devices **48**, 552 (2001).
[7]I. Akasaki and H. Amano, Jpn. J. Appl. Phys., Part 1 **36**, 5393 (1997).
[8]S. A. Smith, C. A. Wolden, M. D. Bremser, A. D. Hanser, R. F. Davis, and W. V. Lampert, Appl. Phys. Lett. **71**, 3631 (1997).
[9]L. Chang, S. Liu, and M. Jeng, Jpn. J. Appl. Phys., Part 1 **40**, 1242 (2001).
[10]Y. K. Yang and T. C. Chang, Microelectron. J. **37**, 746 (2006).
[11]E. Gu, C. W. Jeon, H. W. Choi, G. Rice, M. D. Dawson, E. K. Illy, and M. R. H. Knowles, Thin Solid Films **453–454**, 462 (2004).
[12]W. Liu, R. Zhu, S. Qian, S. Yuan, and G. Zhang, Chin. Phys. Lett. **19**, 1711 (2002).
[13]X. Li, T. Jia, D. Feng, and Z. Xu, Appl. Surf. Sci. **225**, 339 (2004).
[14]A. Piqué, D. B. Chrisey, and C. P. Christensen, in *Direct-Write Technologies for Rapid Prototyping*, edited by A. Piqué and D. B. Chrisey (Academic, San Diego, 2002), pp. 385–414.
[15]M. K. Kelly, O. Ambacher, B. Dahlheimer, G. Groos, R. Dimitrov, H. Angerer, and M. Stutzmann, Appl. Phys. Lett. **69**, 1749 (1996).
[16]T. Akane, T. Sugioka, H. Ogino, H. Takai, and K. Midorikawa, Appl. Surf. Sci. **148**, 133 (1999).
[17]C. B. Schaffer, J. F. Garcia, and E. Mazur, Appl. Phys. A: Mater. Sci. Process. **76**, 351 (2003).
[18]E. G. Gamaly, A. V. Rode, and B. Luther-Davies, J. Appl. Phys. **85**, 4213 (1999).